© 2014. Published by The Company of Biologists Ltd | Journal of Cell Science (2014) 127, 4457–4469 doi:10.1242/jcs.153437

RESEARCH ARTICLE

Galectin-4-mediated transcytosis of transferrin receptor

Andres E. Perez Bay[1], Ryan Schreiner[1], Ignacio Benedicto[1] and Enrique J. Rodriguez-Boulan[1,2,*]

ABSTRACT

Some native epithelia, for example, retinal pigment epithelium (RPE) and kidney proximal tubule (KPT), constitutively lack the basolateral sorting adaptor AP-1B; this results in many basolateral plasma membrane proteins being repositioned to the apical domain, where they perform essential functions for their host organs. We recently reported the underlying apical polarity reversal mechanism: in the absence of AP-1B-mediated basolateral sorting, basolateral proteins are shuttled to the apical plasma membrane through a transcytotic pathway mediated by the plus-end kinesin KIF16B. Here, we demonstrate that this apical transcytotic pathway requires apical sorting of basolateral proteins, which is mediated by apical signals and galectin-4. Using RPE and KPT cell lines, and AP-1B-knockdown MDCK cells, we show that mutation of the N-glycan linked to N727 in the basolateral marker transferrin receptor (TfR) or knockdown of galectin-4 inhibits TfR transcytosis to apical recycling endosomes and the apical plasma membrane, and promotes TfR lysosomal targeting and subsequent degradation. Our results report a new role of galectins in basolateral to apical epithelial transcytosis.

KEY WORDS: Transferrin receptor, Transcytosis, Galectin, Glycan, Rab11a

INTRODUCTION

Epithelial cells perform vectorial transport functions essential for homeostasis that require the polarized distribution of channels, transporters and nutrient receptors into segregated apical and basolateral plasma membrane domains, which are separated by tight junctions (Mellman and Nelson, 2008; Rodriguez-Boulan and Macara, 2014). Many blood nutrients are delivered to epithelial cells through basolateral plasma membrane receptors that are internalized and recycled through defined endosomal compartments. For example, Fe^{3+}-loaded blood transferrin is internalized through basolateral transferrin receptor (TfR) into basolateral sorting endosomes (BSEs) where Fe^{3+} is dissociated by the low pH and translocated to the cytoplasm; Fe^{3+}-free apotransferrin (apoTf), coupled to TfR, recycles back to the cell surface, where the neutral pH causes the release of apoTf to the extracellular medium. Recycling of TfR occurs directly from BSEs (fast recycling loop) or after translocation to perinuclear common recycling endosomes (CREs) (slow recycling loop). Because CREs are reached by both apical and basolateral recycling plasma membrane proteins (Hughson and Hopkins, 1990), TfR recycling from this compartment to the basolateral plasma membrane requires recognition of a basolateral sorting signal in the cytoplasmic tail of TfR by the basolateral sorting adaptor AP-1B (Gravotta et al., 2012; Odorizzi and Trowbridge, 1997). AP-1B is a clathrin-interacting adaptor composed of four subunits (γ, β1, σ1 and μ1B) that is expressed by most columnar epithelia (Ohno et al., 1999) and regulates the sorting of basolateral proteins (Fölsch et al., 1999). However, some native epithelia, for example, the retinal pigment epithelium (RPE) (Diaz et al., 2009) and the kidney proximal tubule (KPT) (Schreiner et al., 2010), lack AP-1B, which results in a dramatic relocation of some cognate basolateral plasma membrane proteins to the apical surface, with important consequences for the physiology of these epithelia.

We recently reported several essential features of this new apical polarity reversal mechanism that operates in AP-1B-deficient epithelia (Perez Bay et al., 2013). Our studies, carried out in AP-1B-knockdown (KD) MDCK cells and in RPE cells (which constitutively lack AP-1B), showed that basolaterally internalized TfR fails to be sorted back to the basolateral plasma membrane at the level of CREs (owing to the absence of AP-1B), and is instead transported from CREs to apical recycling endosomes (AREs) and apical sorting endosomes (ASEs) by the plus-end kinesin KIF16B along non-centrosomal microtubules nucleated by the Golgi apparatus; final delivery to the apical plasma membrane is regulated by the small GTPase Rab11a. A key question that was not addressed by our previous study was whether apical transcytosis of TfR in AP-1B-deficient epithelia requires an apical sorting event, mediated by specific sorting signals and machinery.

N- and O-glycans have been shown to act as apical sorting signals (Fiedler and Simons, 1995; Jacob et al., 2000; Scheiffele et al., 1997; Weisz and Rodriguez-Boulan, 2009; Yeaman et al., 1997) and their recognition by galectin-3, -4 and -9 has emerged as a new apical sorting mechanism (Delacour et al., 2006; Mishra et al., 2010; Stechly et al., 2009). Galectins are synthesized in the cytosol, and secreted by a non-conventional pathway to the apical extracellular space, from where they are subsequently internalized into endosomal compartments and transported back as far as the trans-Golgi network (TGN) (Hughes, 1999; Nickel, 2005). At the TGN or at endosomal compartments, galectins are presumed to bind and sort biosynthetic apical cargo through a pH-dependent cargo clustering mechanism (Straube et al., 2013). In contrast with the established role of galectins in biosynthetic apical sorting, there is no evidence linking them to apical sorting in the transcytotic pathway.

Here, we examined the role of glycans and galectins in transcytosis of TfR using an AP-1B KD approach in MDCK cells, as well as RPE and KTP cell lines that constitutively lack AP-1B. Human TfR contains three N-glycans on N251, N317 and N727 and one O-glycan on T104 (Chen et al., 2009; Hunt et al., 1989). Our experiments show that in AP-1B-deficient epithelia, the N727-glycan operates as an apical sorting signal for TfR apical

[1]Margaret Dyson Vision Research Institute, Weill Medical College of Cornell University, 1300 York Avenue, New York, NY 10065, USA. [2]Department of Cell and Developmental Biology, Weill Medical College of Cornell University, 1300 York Avenue, New York, NY 10065, USA.

*Author for correspondence (boulan@med.cornell.edu)

Received 18 March 2014; Accepted 5 August 2014

Journal of Cell Science

Journal of Cell Science (2014) 127, 4457–4469 doi:10.1242/jcs.153437

transcytosis via AREs, whereas the sorting lectin galectin-4 is also required for this pathway. Functional ablation of either the N727 apical signal or galectin-4 inhibited apical transcytosis of TfR and increased its lysosomal degradation. Hence, we demonstrate that apical relocation of basolateral proteins in AP-1B-deficient epithelia requires apical sorting signals and report the first role of galectins in epithelial transcytosis.

RESULTS

N-glycan linked to N727 mediates apical localization of TfR in AP-1B KD MDCK cells

To study the possible role of N- and O-glycans in the sorting of TfR, we performed alanine mutagenesis of T104 and N251, N317 and N727 in TfR tagged at C-terminal end with GFP. Because TfR is a type II plasma membrane protein, GFP faces the extracellular medium in the expressed protein. Then, we studied the polarized distribution of these mutant TfRs after lipofectamine-based expression of their cDNAs into wild-type (WT) and AP-1B KD MDCK cells. Briefly, we plated the cells at full confluence on Transwell filters, transfected them 3 days later with GFP-tagged WT, or with the GFP-tagged T104A, N251A, N317A or N727A TfR, and examined them at day 4. After paraformaldehyde fixation, rabbit antibody against GFP was applied to both apical and basolateral chambers. To discriminate between apical and basolateral TfR–GFP, secondary goat anti-rabbit-IgG antibodies labeled with Alexa Fluor 568 (red pseudocolor) or Alexa Fluor 647 (green pseudocolor) were applied to the apical or basolateral chamber, respectively.

Fig. 1A shows that, in WT MDCK cells, WT and all four mutant TfR–GFP proteins were basolaterally localized, as shown by the robust green basolateral fluorescence signal and the negligible apical red fluorescence signal. In contrast, in AP-1B KD MDCK cells, GFP-tagged WT, T104A, N251A and N317A TfR displayed strong apical red fluorescent signal, consistent with their apical transcytosis (Perez Bay et al., 2013). Strikingly, N727A-TfR-–GFP remained mostly basolateral in AP-1B KD MDCK cells, indicating that this mutant TfR is not transcytosed to the apical plasma membrane in these cells. Quantitative analysis confirmed that the apical:basolateral ratio of WT-TfR–GFP was seven times higher in AP-1B KD MDCK compared to

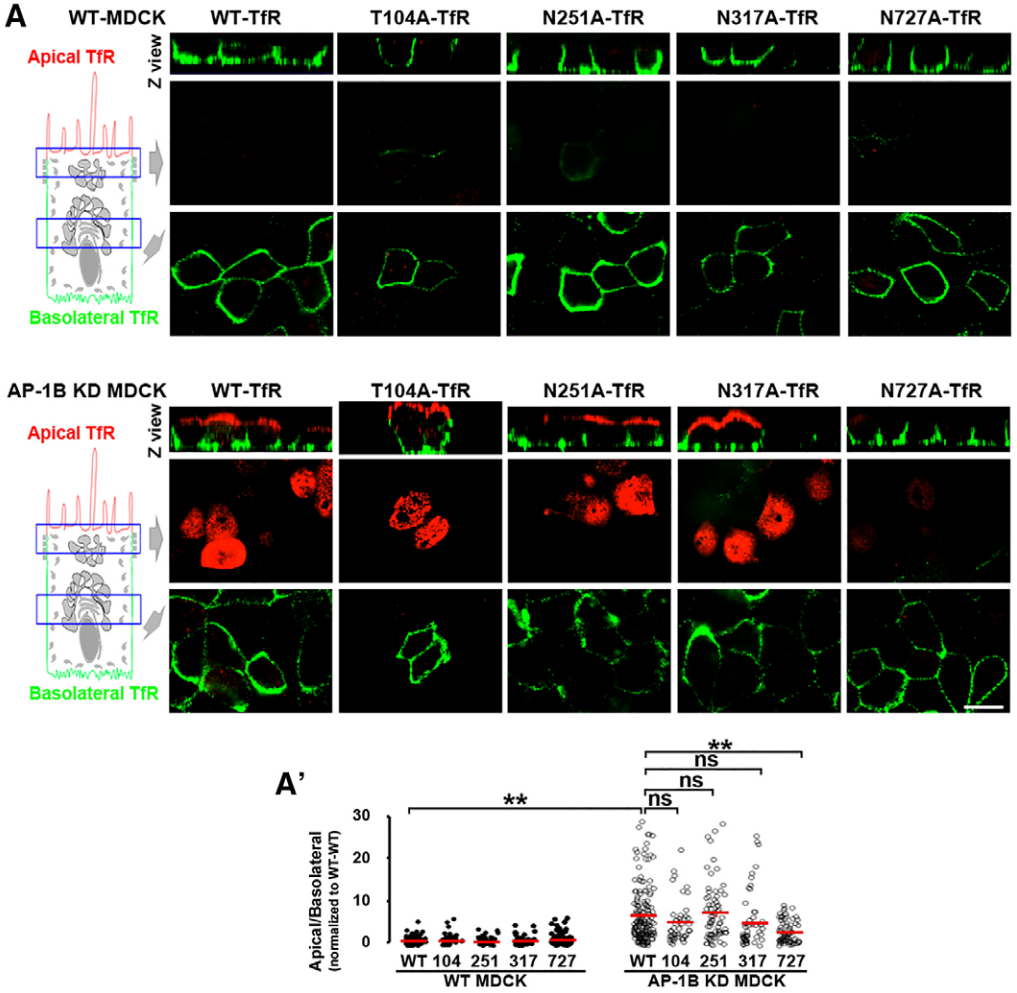

Fig. 1. The N-glycan linked to N727 mediates apical localization of TfR in AP-1B KD MDCK cells. (A) Polarized WT (top) and AP-1B KD (bottom) MDCK cells were transiently transfected with either WT- or TfR–GFP mutated in each of its four glycosylation sites. Cells were immunostained for surface TfR–GFP (without permeabilizing the cells) using rabbit anti-GFP primary antibody and secondary anti-rabbit-IgG antibodies labeled with Alexa Fluor 568 (red) or 647 (green) in the apical and basolateral chambers, respectively. (A′) Cells from experiments represented in A were quantified for the apical:basolateral ratio using the fluorescence signal of each plasma membrane domain. Circles correspond to individual cells obtained from different experiments and red lines indicate the mean. ns, not significant, ** $P<0.001$. Scale bar: 10 μm.

Journal of Cell Science (2014) 127, 4457–4469 doi:10.1242/jcs.153437

WT MDCK cells (7.2±0.5 vs 1±0.1, mean±s.e.m, $P<0.001$). Importantly, the apical:basolateral ratio of N727A-TfR–GFP was significantly lower than WT-TfR–GFP in AP-1B KD MDCK cells (3±0.3, $P<0.001$) (Fig. 1A′).

Our approach of detecting apical and basolateral TfR–GFP in the same cells has higher accuracy than when applying antibodies to the apical or basolateral chambers of different Transwell filters; however, the value of apical:basolateral ratio obtained is relative because different fluorophores are used. To obtain absolute values of this ratio, we applied rabbit anti-GFP antibody prelabeled with the fluorophore SeTau647 to either the apical or basolateral chambers of separate Transwell filters (supplementary material Fig. S1a,a′). We found that the apical:basolateral ratio of WT-TfR–GFP was four times higher in AP-1B KD MDCK (63%±12) than in WT MDCK cells (16%±5, $P<0.001$) and the apical:basolateral ratio of N727A-TfR–GFP was almost half (35%±7, $P<0.05$) of WT-TfR–GFP in AP-1B KD MDCK cells.

The reduced apical:basolateral ratio of N727A-TfR–GFP was not caused by: (1) lower total expression of TfR, as microscopy and western blot experiments indicated that expression of this protein was not reduced compared to WT-TfR–GFP (see Figs 3 and 4); or (2) retention in the endoplasmic reticulum, as this mutant was expressed at high levels in the basolateral membrane of both WT and AP-1B KD MDCK cells. In contrast, a TfR–GFP mutated in all four TfR glycosylation sites did not reach the apical or basolateral plasma membrane (supplementary material Fig. S1b,c).

Taken together, the results in this section suggest that the N-glycan linked to N727 functions as an apical sorting signal that mediates apical localization of TfR in AP-1B-deficient epithelia.

The N-glycan linked to N727 mediates apical transcytosis of TfR in AP-1B KD MDCK cells

The experiments described above indicated that the N727-linked glycan acts as an apical sorting signal for TfR in AP-1B KD MDCK cells but did not inform on whether this sorting event is required for transcytosis of the receptor. To directly study the role of the N727-linked glycan in TfR transcytosis, we transiently transfected WT and AP-1B KD MDCK cells with WT or N727A-TfR–GFP and measured apical transcytosis of these proteins by labeling the basolateral pool of the proteins with SeTau647-labeled rabbit anti-GFP antibodies (120 min, 4℃) and following its translocation to the apical surface at different times after a temperature switch to 37℃ through the apical addition of Alexa-Fluor-568-conjugated goat anti-rabbit-IgG antibodies. This experiment showed that whereas WT MDCK cells transcytosed neither WT nor N727A-TfR–GFP (Fig. 2A), AP-1B KD MDCK cells transcytosed WT-TfR–GFP but only a reduced fraction of N727A-TfR–GFP (Fig. 2B). Quantification of the results indicated that ratio of the Alexa Fluor 568 signal to the SeTau647 signal, which is proportional to the fraction of basolaterally internalized SeTau647-labeled rabbit anti-GFP antibody transcytosed to the apical plasma membrane, was significantly higher for WT-TfR–GFP than in N727A-TfR–GFP (100%±21 vs 34%±3, mean±s.e.m., $P<0.001$) at 30 min in AP-1B KD MDCK cells (Fig. 2A′,B′). As a control, no transcytosis signal was observed if SeTau647-labeled rabbit anti-GFP antibody was not added to the basolateral side (Fig. 2A,B, right-hand column). An additional control indicated that incubation of MDCK cells with basolateral SeTau647-labeled rabbit anti-GFP antibody and apical Alexa-Fluor-568-conjugated goat anti-rabbit-IgG at 4℃ for 60 min resulted in no apical Alexa Fluor 568 signal (Fig. 2A,B, left column), ruling out the possibility that fluorescent antibodies might diffuse paracellularly between the apical and basolateral chambers. Only cells transfected with WT- or N727-TfR–GFP bound fluorescent antibodies, as confirmed by the GFP signal of the cells shown in Fig. 2 (see also supplementary material Fig. S2a,b).

Taken together, these results indicate that the N727-linked glycan mediates an apical sorting event required for apical transcytosis of TfR in AP-1B-deficient epithelia.

The N-glycan linked to N727 mediates TfR trafficking to ARE in AP-1B KD MDCK cells

We previously reported that TfR apical transcytosis in AP-1B KD MDCK and RPE cells occurs via Rab11a-positive AREs (Perez Bay et al., 2013). Is the N727-linked glycan necessary for transport of TfR to AREs? To investigate this question, we examined the colocalization of TfR–GFP with endogenous Rab11a (an ARE marker) in WT and AP-1B KD MDCK cells. As expected, neither WT-TfR–GFP nor any of the single glycan-deleted receptor mutants colocalized with Rab11a in WT MDCK cells, consistent with the fact that AP-1B promotes basolateral recycling of TfR in these cells. In contrast, GFP-tagged WT, T104A, N251A and N317A TfR displayed a robust colocalization with Rab11a in AP-1B KD MDCK cells, consistent with their utilization of AREs as an endosomal relay station during transcytosis (Fig. 3). Quantitative analysis confirmed the significantly higher Manders' colocalization coefficients of Rab11a with TfR–GFP (MCC1), and TfR–GFP with Rab11a (MCC2) in AP-1B KD MDCK compared to WT MDCK cells (Fig. 3A′). Strikingly, N727A-TfR–GFP exhibited significantly lower MMC1 and MCC2 values than WT-TfR–GFP ($P<0.001$) in AP-1B KD MDCK, owing to reduced trafficking of this mutant TfR to AREs (Fig. 3A′). Interestingly, N317A-TfR–GFP also displayed significantly lower MCC1 and MCC2 values in AP-1B KD MDCK cells, relative to WT-TfR–GFP ($P<0.05$), suggesting that this N-glycan has a minimal role in transcytosis of TfR that cannot be detected with the full transcytosis assay utilized in the previous section.

The results in this section further strengthen the conclusion that the N727-linked glycan mediates TfR transcytosis to the apical membrane via AREs.

N727A-TfR recycles inefficiently to the basolateral membrane and is targeted for lysosomal degradation in AP-1B KD MDCK cells

What is the fate of N727A-TfR–GFP in AP-1B KD MDCK cells? Is it retained intracellularly, relocated to the basolateral plasma membrane or targeted for lysosomal degradation? First, we investigated whether N727A-TfR–GFP is retained intracellularly, by determining the surface:total ratio of WT-TfR–GFP and N727A-TfR–GFP in AP-1B KD MDCK cells grown on Transwell filters. The surface localization (apical plus basolateral) of TfR–GFP was measured by applying successively primary rabbit anti-GFP antibody and secondary Alexa-Fluor-568-conjugated goat anti-rabbit-IgG antibody to both the apical and basolateral chambers, whereas the total TfR–GFP signal was measured simply from the GFP fluorescence. These experiments demonstrated that WT- and N727A-TfR–GFP displayed a similar surface:total ratio in AP-1B

Journal of Cell Science (2014) 127, 4457–4469 doi:10.1242/jcs.153437

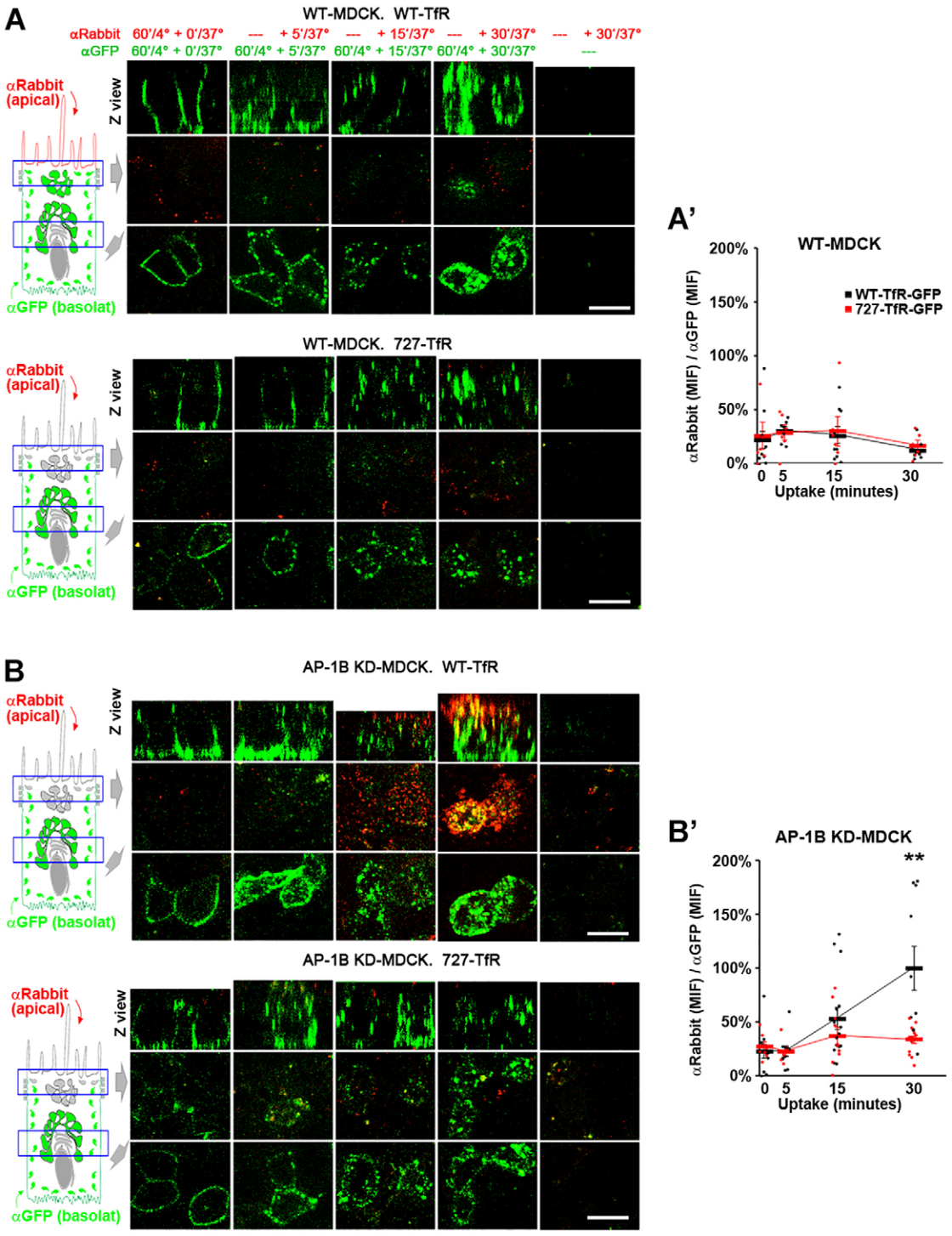

Fig. 2. The N-glycan linked to N727 mediates apical transcytosis of TfR in AP-1B KD MDCK cells. Polarized WT (A) and AP-1B KD (B) MDCK cells were transiently transfected with either WT (top) or N727A (bottom) TfR–GFP. SeTau647-labeled rabbit anti-GFP antibodies (αGFP, green) were applied to the basolateral chamber (120 min, 4˚C) to allow basolateral surface binding. The temperature was shifted to 37˚C to allow antibody uptake and transcytosis for the indicated times periods, during which time the Alexa-Fluor-568-conjugated anti-rabbit-IgG antibody (αRabbit, red) was applied to the apical chamber. (A′,B′) Cells from experiments represented in A and B were quantified for the 'αRabbit (MIF):αGFP (MIF) ratio, which is proportional to the fraction of basolateral SeTau647-labeled rabbit anti-GFP antibody transcytosed to the apical plasma membrane. Values were normalized to the highest value (i.e. 30 min uptake in AP-1B KD MDCK with WT-TfR–GFP). Circles correspond to individual cells obtained from different experiments and thick lines indicate the mean±s.e.m. $^{**}P<0.001$. Scale bars: 10 μm.

KD MDCK cells (Fig. 4A,A′), indicating that N727A-TfR–GFP is not retained intracellularly. Next, we studied whether N727A-TfR–GFP is relocated to the basolateral plasma membrane in AP-1B KD MDCK cells, by determining the basolateral:total ratio (in this experiment Alexa-Fluor-568-conjugated goat anti-rabbit-IgG was applied only to the basolateral chamber). N727A-TfR–GFP displayed a slightly, yet significantly, higher basolateral:surface ratio compared to WT-TfR–GFP (1.28±0.16 vs 1±0.06,

Journal of Cell Science (2014) 127, 4457–4469 doi:10.1242/jcs.153437

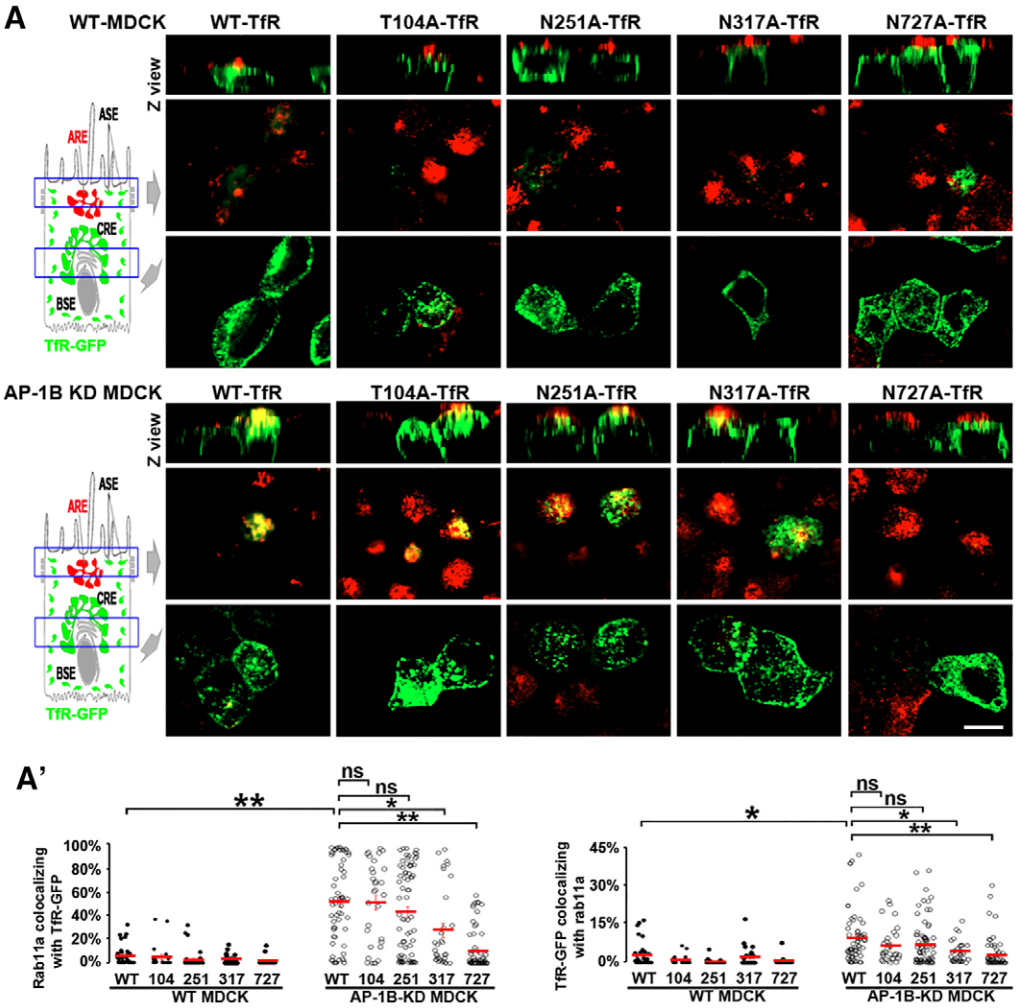

Fig. 3. The N-glycan linked to N727 mediates TfR trafficking to ARE in AP-1B KD MDCK cells. (A) Polarized WT (top) and AP-1B KD (bottom) MDCK cells were transiently transfected with either WT or mutant TfR–GFP in each of its four glycosylation sites, and immunostained for Rab11a. (A′) Cells from experiments represented in A were quantified for the percentage of pixels of Rab11a colocalizing with TfR–GFP (left) and the percentage of pixels of TfR–GFP colocalizing with Rab11a (right). Circles correspond to individual cells obtained from different experiments and red lines indicate the mean. ns, not significant; *$P<0.05$; **$P<0.001$. Scale bar: 10 µm.

mean±s.e.m., $P<0.05$) (Fig. 4B,B′), indicating that lack of the N727-linked glycan signal promotes inefficient AP-1B-independent recycling of TfR to the basolateral plasma membrane in AP-1B KD MDCK cells.

Other experiments indicated that N727A TfR was targeted for lysosomal degradation in AP-1B KD MDCK cells. For these experiments, we measured the internalization of transiently transfected WT or N727A TfR, tagged at the extracellular C-terminus with HA, in AP-1B KD MDCK cells. The basolateral pool of these proteins was labeled with basolateral incubation of SeTau647-labeled mouse anti-HA antibody (120 min, 4℃) and its trafficking to lysosomes was measured through its colocalization with the lysosomal marker Lamp1 at different times after the switch to 37℃. As expected, internalized N727A-TfR–HA did not colocalize with Lamp1 at early uptake times (0 and 5 min); however, after 30 min uptake, a substantial amount of N727A-TfR–HA colocalized with Lamp1 (Fig. 4C); in contrast, basolaterally internalized WT-TfR–HA colocalized poorly with the lysosomal marker Lamp1 at all time points studied. Quantitative analysis confirmed that the colocalization of SeTau647-labeled mouse anti-HA antibody with Lamp1 (MCC1), as well as Lamp1 with SeTau647-labeled mouse anti-HA antibody (MCC2), was significantly higher for N727A compared to WT-TfR–HA at 30 min (9%±1 vs 18%±3, $P<0.01$; and 10%±2 vs 17%±2, $P<0.05$) (Fig. 4C′).

For the experiments just described, we did not use TfR–GFP because the antibodies against GFP and Lamp1 are both rabbit antibodies. To confirm the result obtained in these experiments using the same TfR–GFP constructs used in previous experiments, lysosomes were labeled with a 60-min uptake of 10-kDa dextran followed by an additional 60-min chase in subconfluent WT and AP-1B KD MDCK cells. WT-TfR–GFP colocalized poorly with this lysosomal marker in both WT and AP-1B KD MDCK cells, whereas N727A-TfR–GFP displayed a slightly higher colocalization in WT MDCK cells. Strikingly, N727A-TfR–GFP displayed strong colocalization with this lysosomal marker in AP-1B KD MDCK cells, which was significantly higher than that of WT MDCK cells (supplementary material Fig. S2c,c′).

Finally, if lack of AP-1B promoted lysosomal degradation of N727A-TfR–GFP, it would be expected that the expression levels of this protein would be decreased in AP-1B KD MDCK cells relative to those of WT-TfR–GFP. Indeed, this is what we observed by western blot analysis of cycloheximide-treated WT and AP-1B KD MDCK cells (Fig. 4D). Whereas the expression level of WT-TfR–GFP was not reduced after 8 h of cycloheximide treatment in both WT and AP-1B KD MDCK cells, the expression of N727A-TfR–GFP in cycloheximide-treated WT MDCK cells displayed a significant reduction to

Journal of Cell Science (2014) 127, 4457–4469 doi:10.1242/jcs.153437

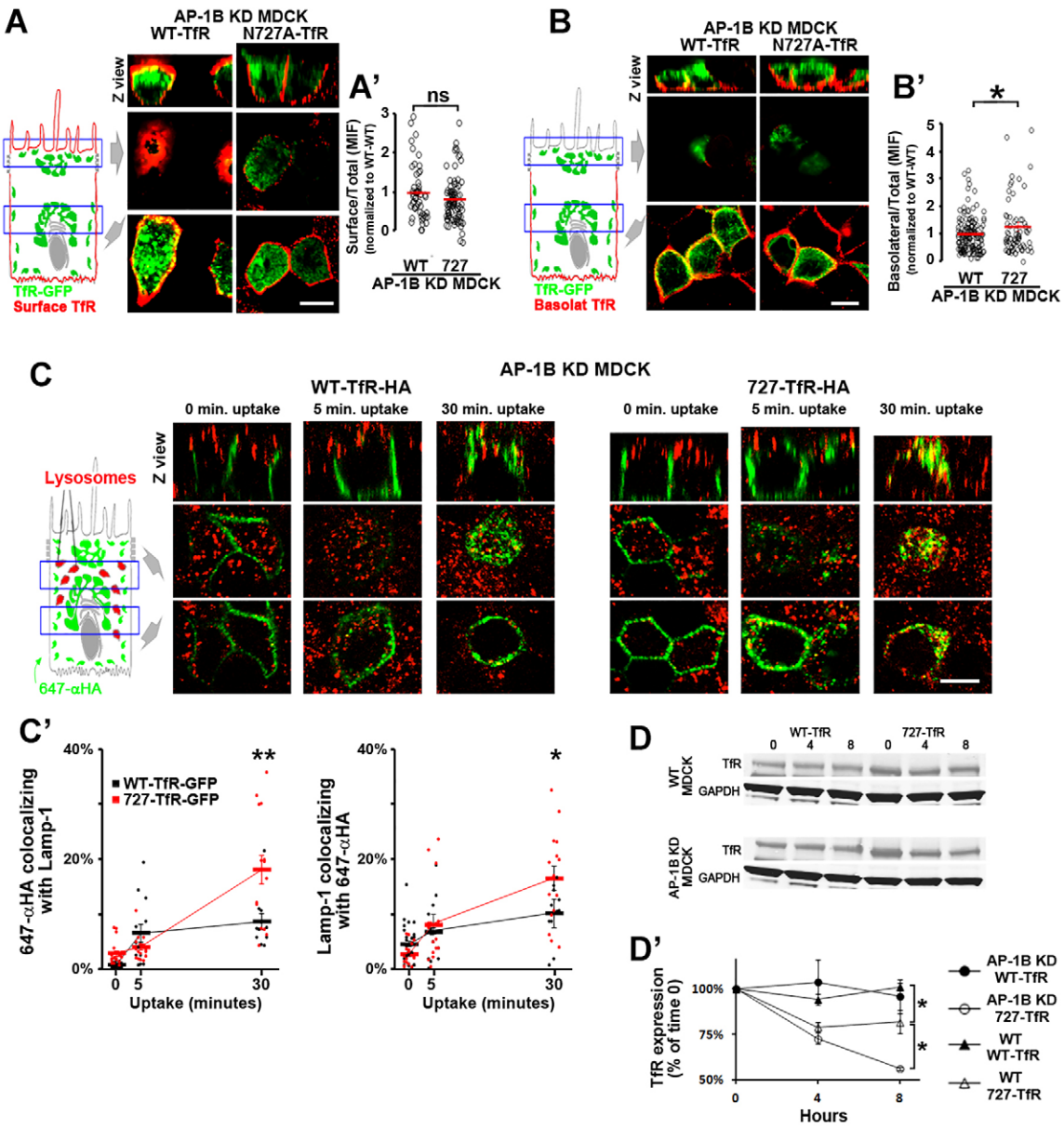

Fig. 4. N727A TfR recycles inefficiently to the basolateral membrane and is targeted for lysosomal degradation in AP-1B KD MDCK cells. (A) Polarized AP-1B KD MDCK cells were transiently transfected with either WT- or N727A-TfR–GFP and were immunostained for surface TfR–GFP (without permeabilizing the cells), with primary rabbit anti-GFP (green) and secondary Alexa-Fluor-568-conjugated anti-rabbit-IgG (red) antibodies applied to both the apical and basolateral chambers. (A′) Cells from experiments represented in A were quantified for the surface:total ratio using the fluorescent signals of Alexa-Fluor-568-conjugated anti-rabbit-IgG (surface) and GFP (total). (B) Polarized AP-1B KD MDCK cells were transiently transfected with either WT- or N727A-TfR–GFP and immunostained for basolateral TfR–GFP only. (B′) Cells from experiments represented in B were quantified for the basolateral:total ratio using the fluorescent signals of Alexa-Fluor-568-conjugated anti-rabbit-IgG (basolateral) and GFP (total). (C) Polarized AP-1B KD MDCK cells were transiently transfected with either WT- or N727A-TfR–HA. SeTau647-labeled anti-HA antibody (647-αHA, green) was bound to the basolateral plasma membrane (120 min, 4˚C), the temperature was shifted to 37˚C to allow antibody uptake and cells were fixed at the indicated times periods and immunostained for the lysosomal marker Lamp1. (C′) Cells from experiments represented in C were quantified for the percentage of pixels of 647-αHA colocalizing with Lamp1 (left) and the percentage of pixels of Lamp1 colocalizing with 647-αHA (right), for each time point studied. (D) WT and AP-1B KD MDCK cells were nucleofected with either WT- or N727A-TfR–GFP, treated with cycloheximide for the indicated time periods and analyzed for TfR–GFP expression by western blotting. (D′) Quantitative analysis of WT- and N727A-TfR–GFP in three or four experiments represented in D. Circles correspond to individual cells obtained from different experiments and thick lines indicate the mean±s.e.m. for C′ and D′. ns, not significant; * $P<0.05$; ** $P<0.01$. Scale bars: 10 μm.

82%±4 ($P<0.05$) (Fig. 4D,D′). Strikingly, N727A-TfR–GFP degradation was significantly higher in AP-1B KD MDCK cells compared to WT MDCK cells (56%±1 vs 82%±4, $P<0.01$) (Fig. 4D,D′),

Taken together, these results demonstrate that the reduced apical transcytosis of the N727A TfR in AP-1B KD MDCK cells, results in increased basolateral recycling independent of AP-1B and in increased lysosomal targeting and degradation.

Journal of Cell Science

Journal of Cell Science (2014) 127, 4457–4469 doi:10.1242/jcs.153437

Galectin-4 prevents lysosomal targeting of basolaterally internalized TfR and promotes its apical transcytosis via ARE in AP-1B KD MDCK cells

Galectin-3 and galectin-4 are expressed in MDCK cells and have been implicated in biosynthetic apical trafficking (Delacour et al., 2006; Poland et al., 2011; Stechly et al., 2009); however, their possible roles in apical transcytosis have not been studied. To investigate whether any of these lectins mediate apical transcytosis of TfR, we generated AP-1B KD MDCK cells stably expressing the human WT TfR (AP-1B KD/TfR MDCK, clone 10.4), silenced galectin-3 and/or galectin-4 using small interfering RNA (siRNA) and studied the polarized distribution of TfR with surface immunofluorescence (Fig. 5). Western blot and RT-PCR analysis was used to establish the silencing efficiency of galectin-3 and 4, respectively, because antibodies were only available for galectin-3 (Fig. 5B). The silencing of medium subunit μ1B of AP-1B was established by RT-PCR (Fig. 5C). Galectin-4 KD caused a significant reduction of apical TfR in AP-1B KD MDCK cells, whereas galectin-3 KD had no effect (Fig. 5A). Simultaneous silencing of both galectins did not cause an additive effect compared to galectin-4 KD alone (Fig. 5A). Quantitative analysis confirmed that the apical:basolateral ratio of TfR decreased from 1±0.13 in luciferase KD to 0.67±0.06 (mean±s.e.m., $P<0.05$) in galectin-4 KD and 0.54±0.05 ($P<0.001$) in the galectin-3/galectin-4 double KD. By contrast, galectin-3 KD did not reduce the apical/basolateral ratio of TfR (1±0.08) (Fig. 5A′). Identical results were obtained with a second clone of AP-1B KD/TfR MDCK cells (clone 4.23) (supplementary material Fig. S3a,a′). Galectin-4 KD did not alter the overall polarity of MDCK cells, as knockdown of this galectin did not affect the basolateral localization of TfR–GFP proteins in WT MDCK or N727A-TfR–GFP in AP-1B KD MDCK cells (supplementary material Fig. S3b–b″).

To study the fate of basolaterally internalized TfR (i.e. transport to AREs or lysosomes) in AP-1B KD/TfR MDCK cells knocked down for galectin-3 and galectin-4, CF594-labeled Tf (CF594–Tf) was applied basolaterally (30 min, 37℃), followed by immunostaining of AREs and lysosomes. Fig. 6A shows that galectin-4 KD (but not galectin-3 KD) reduced the colocalization of basolaterally internalized CF594–Tf and the ARE marker Rab11a compared to luciferase KD in AP-1B KD/TfR MDCK cells. Quantitative analysis in luciferase, galectin-3 KD and galectin-4 KD cells indicated that the colocalization of Rab11a with CF594–Tf (MCC1) was 58%±5, 56%±6 and 15%±3 (mean±s.e.m., $P<0.001$) and the colocalization of CF594–Tf with Rab11a (MCC2) was 7%±1, 6%±1 and 2%±1 ($P<0.001$) (Fig. 6A′). In contrast, galectin-4 KD (but not galectin-3 KD) increased the colocalization of basolaterally

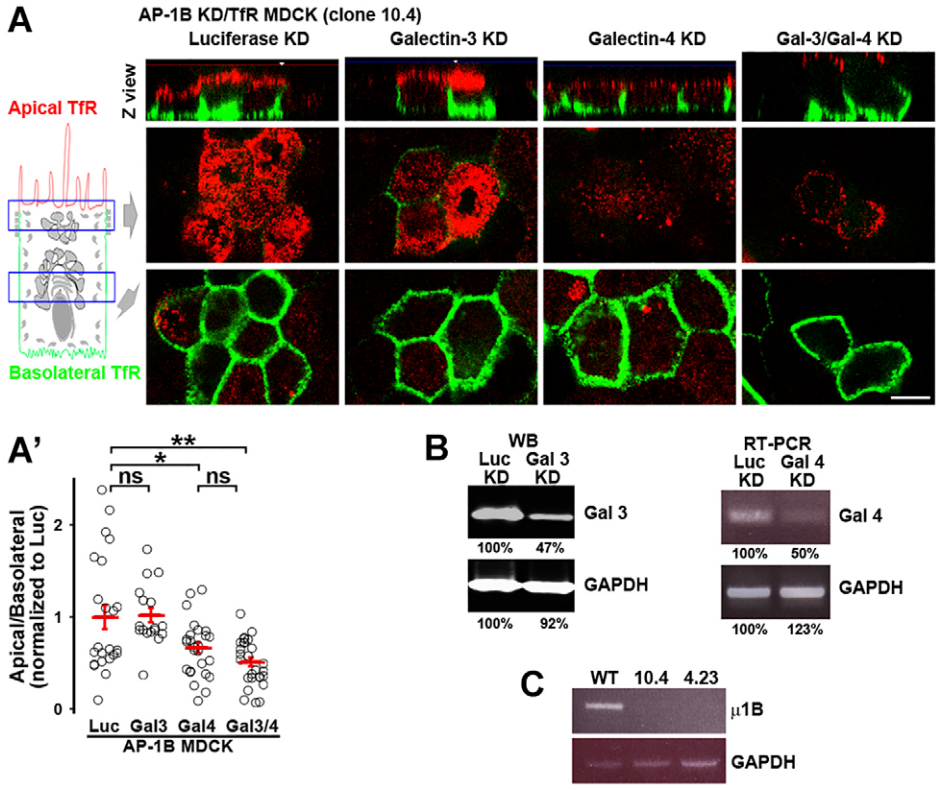

Fig. 5. Galectin-4 mediates apical localization of TfR in AP-1B KD MDCK cells. (A) AP-1B KD MDCK cells stably expressing human TfR (AP-1B KD/TfR MDCK) were knocked down for luciferase (Luc), galectin-3 (Gal 3), galectin-4 (Gal 4), or both galectin-3 and galectin-4 (Gal3/4) and polarized on transwell filters. Apical and basolateral TfR was immunostained (without permeabilizing the cells), using anti-human-TfR primary antibody that recognizes the luminal domain of TfR and Alexa-Fluor-568-conjugated anti-mouse-IgG (red) and Alexa-Fluor-647-conjugated anti-mouse-IgG (green) secondary antibodies in the apical and basolateral chambers, respectively. (A′) Cells from experiments represented in A were quantified for the apical:basolateral ratio using the fluorescence signal of each plasma membrane domain. (B) Western blot (WB) analysis of galectin-3 expression, and RT-PCR analysis of galectin-4 expression in AP-1B KD/TfR MDCK cells electroporated with siRNA against luciferase, galectin-3 or galectin-4. A quantification of protein levels is presented below the blot. (C) RT-PCR analysis of μ1B expression (the medium subunit of AP-1B) in WT MDCK and the two AP-1B KD/TfR MDCK clones used in this work. Circles correspond to individual cells obtained from different experiments and red lines indicate the mean±s.e.m. ns, not significant; *$P<0.05$; **$P<0.001$. Scale bar: 10 μm.

Journal of Cell Science (2014) 127, 4457–4469 doi:10.1242/jcs.153437

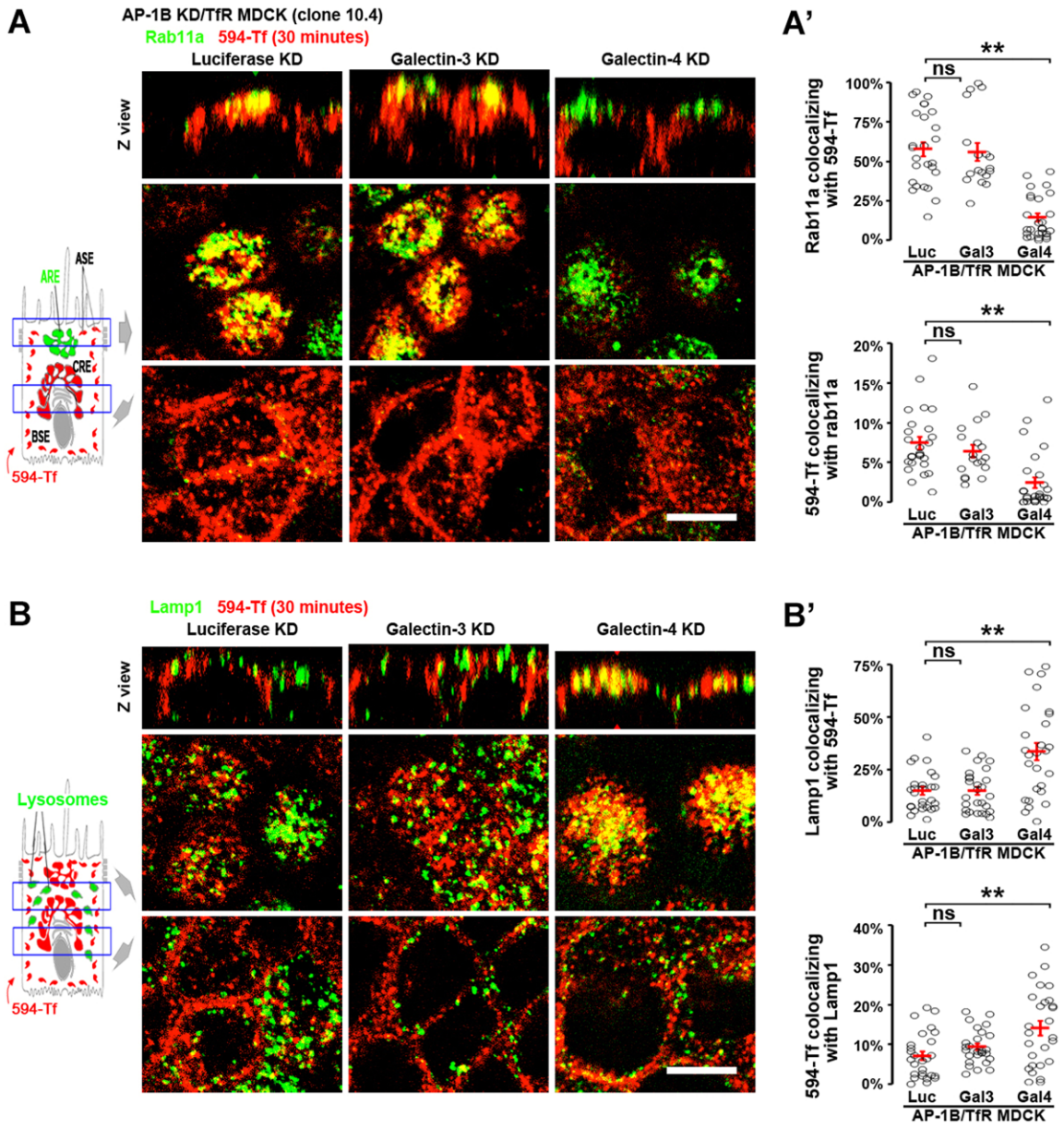

Fig. 6. Galectin-4 promotes ARE trafficking and prevents lysosomal targeting of basolaterally internalized TfR in AP-1B KD MDCK cells. AP-1B KD/TfR MDCK cells were knocked down for luciferase (Luc), galectin-3 (Gal3) or galectin-4 (Gal4) and polarized on transwell filters. Cells were incubated basolaterally with CF594–Tf (594-Tf, red) for 30 min and subsequently stained for the ARE marker Rab11a (A) or the lysosomal marker Lamp1 (B) (green). (A′) Cells from experiments represented in A were quantified for the percentage of pixels of Rab11a colocalizing with CF594–Tf (top) and the percentage of pixels of CF594–Tf colocalizing with Rab11a (bottom). (B′) Cells from experiments represented in B were quantified for the percentage of pixels of Lamp1 colocalizing with CF594–Tf (top) and the percentage of pixels of CF594–Tf colocalizing with Lamp1 (bottom). Circles correspond to individual cells obtained from different experiments and red lines indicate the mean±s.e.m. ns, not significant; $^{**}P<0.001$. Scale bars: 10 μm.

internalized CF594–Tf and the lysosomal marker Lamp1 compared to luciferase KD in AP-1B KD/TfR MDCK cells (Fig. 6B). Quantitative analysis in luciferase, galectin-3 KD and galectin-4 KD cells indicated that the colocalization of Lamp1 with CF594–Tf (MCC1) was 15%±2, 15%±2 and 34%±4 ($P<0.001$) and the colocalization of CF594–Tf with Lamp1 (MCC2) was 7%±1, 9%±1 and 14%±2 ($P<0.001$) (Fig. 6B′).

Because N-glycans have been implicated in the transcytosis of polymeric IgA receptor (pIgR) (Luton et al., 2009), we studied whether galectin-3 and galectin-4 were involved in this process. Strikingly, neither galectin-3 nor galectin-4 silencing inhibited apical transcytosis of the pIgR (supplementary material Fig. S4), suggesting that multiple transcytotic pathways coexist in MDCK cells.

Taken together, these results indicate that galectin-4 mediates TfR apical transcytosis in AP-1B KD MDCK cells, by promoting its trafficking to ARE and preventing its lysosomal targeting.

The N727-linked glycan signal and galectin-4 sorting machinery operate in constitutively AP-1B-deficient epithelial cells

The RPE and the KPT constitutively lack the major basolateral sorting adaptor AP-1B and express several basolateral proteins in the apical plasma membrane. Therefore, we studied whether the

Journal of Cell Science (2014) 127, 4457–4469 doi:10.1242/jcs.153437

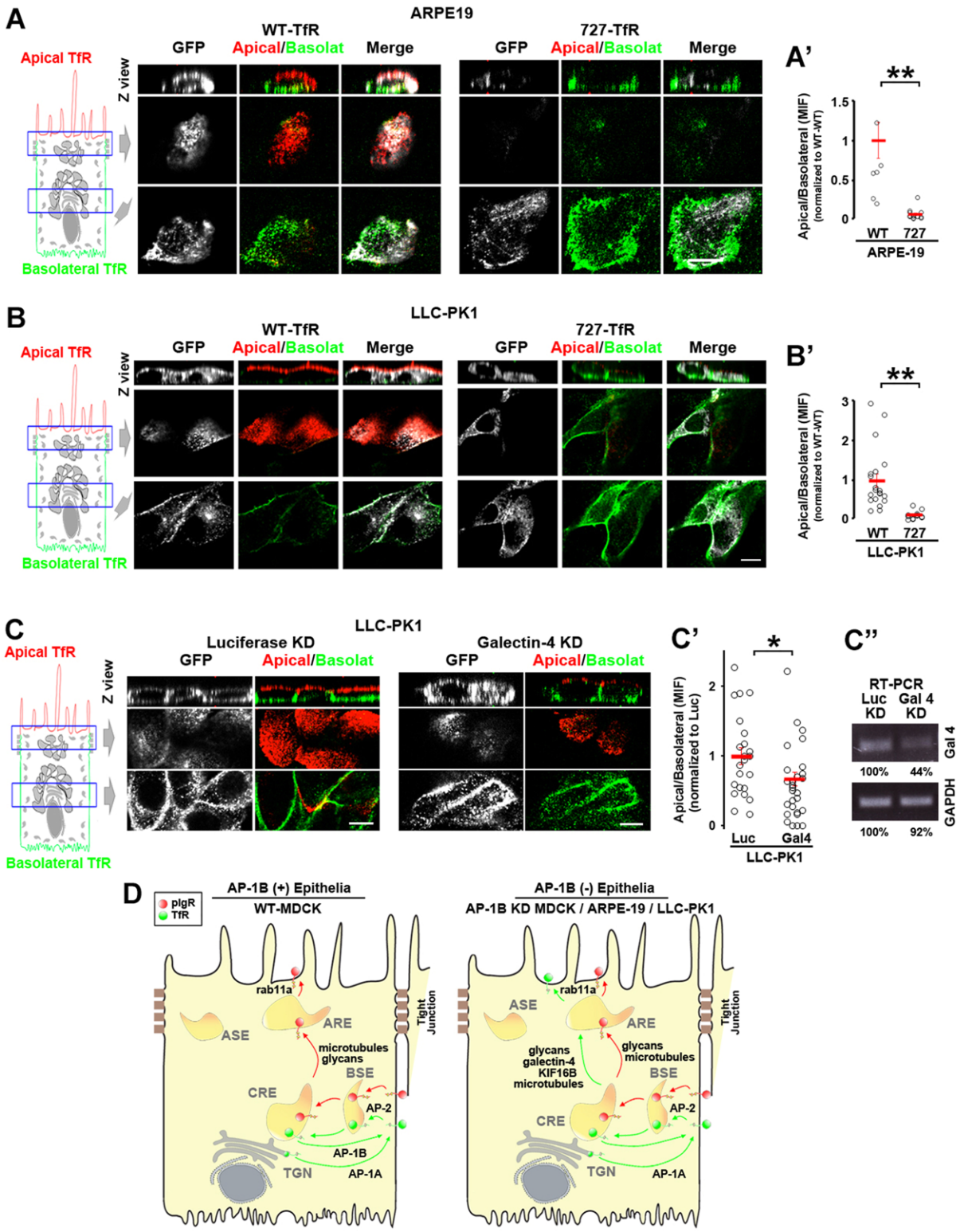

Fig. 7. See next page for legend.

N727-glycan signal and galectin-4 are required for TfR apical localization in RPE and KPT cell lines (i.e. ARPE-19 and LLC-PK1, respectively). Fig. 7 shows that WT-TfR–GFP localized to both apical and basolateral surfaces of ARPE-19 (Fig. 7A) and LLC-PK1 (Fig. 7B) cells, whereas N727A-TfR–GFP was mostly basolateral. Quantitative analysis confirmed that the apical:basolateral ratio of WT-TfR–GFP was significantly higher than that of N727A-TfR–GFP ($P<0.001$) in both cell

Journal of Cell Science (2014) 127, 4457–4469 doi:10.1242/jcs.153437

Fig. 7. The N727-glycan signal/galectin-4 sorting machinery operates in constitutively AP-1B-deficient epithelial cells. (A) Polarized ARPE-19 (A) and LLC-PK1 cells were transiently transfected with either WT- or N727A-TfR–GFP. Cells were immunostained for surface TfR–GFP (without permeabilizing the cells) using anti-GFP primary antibody and Alexa-Fluor-568-conjugated anti-rabbit-IgG (red) and Alexa-Fluor-647-conjugated anti-rabbit-IgG (green) secondary antibodies in the apical and basolateral chambers, respectively. (A′,B′) Cells from experiments represented in A and B were quantified for the apical:basolateral ratio using the fluorescence signal of each plasma membrane domain. (C) LLC-PK1 cells were knocked down for luciferase (Luc) or galectin-4 and polarized on transwell filters. Apical and basolateral TfR was immunostained in the same manner as above. (C′) Cells from experiments represented in C were quantified for the apical:basolateral ratio using the fluorescence signal of each plasma membrane domain. (D) Model. Polarized WT MDCK cells display TfR basolateral recycling mediated by the clathrin adaptor AP-1B and apical transcytosis of pIgR. In contrast AP-1B-deficient epithelial cells, such as AP-1B KD MDCK, ARPE-19 and LLC-PK1, transcytose a substantial fraction of TfR to the apical plasma membrane via AREs, mediated by the N727-linked glycan signal, galectin-4, Rab11a, microtubules and the microtubule motor KIF16B. Circles correspond to individual cells obtained from different experiments and red lines indicate the mean±s.e.m. *$P<0.05$, **$P<0.001$. Scale bars: 10 μm.

lines (Fig. 7A′,B′). Furthermore, galectin-4 KD in LLC-PK1 cells significantly reduced the amount of apical WT-TfR–GFP compared to luciferase KD (Fig. 7C,C′).

These results indicate that the N727-linked glycan signal and galectin-4 mediate TfR apical sorting in epithelial cells that are constitutively deficient in AP-1B.

DISCUSSION

Extensive studies over the past 15 years have characterized the important roles played by clathrin and the clathrin adaptor AP-1B in basolateral sorting in epithelial cells (Bonifacino, 2014; Fölsch et al., 1999; Gonzalez and Rodriguez-Boulan, 2009; Rodriguez-Boulan et al., 2013). However, it has also become clear that some epithelia (e.g. RPE and KPT) lack this adaptor and require their apically relocated basolateral proteins to carry out homeostatic functions for the host organs, that is, the retina and kidney (Diaz et al., 2009; Ohno et al., 1999; Schreiner et al., 2010). In this report and in a previous publication (Perez Bay et al., 2013), we have investigated the mechanisms responsible for the apical relocation of cognate basolateral recycling receptors in AP-1B-deficient epithelia. According to the model supported by these studies (Fig. 7D), the absence of AP-1B promotes the incorporation of the basolateral proteins into a transcytotic pathway from CREs to AREs and ASEs that is mediated by the plus-end kinesin motor KIF16B and non-centrosomal Golgi-originated microtubules. The transcytosed proteins require Rab11a for delivery to the apical membrane. Here, we identify two additional key features of this mechanism, that is, the role of N727-linked glycan in TfR as an apical sorting signal and the role of galectin-4 as an apical sorter in the transcytotic pathway. Although galectins have been shown to mediate apical sorting in the biosynthetic pathway, this study provides the first evidence for a role of galectins in the apical transcytotic pathway.

Implications for apical-basolateral sorting in epithelia

Our results are consistent with current models on apical-basolateral sorting in epithelia that posit that, in general, apical sorting signals are recessive relative to basolateral sorting signals (Fölsch, 2008; Mostov et al., 2000; Rodriguez-Boulan et al., 2005; Weisz and Rodriguez-Boulan, 2009). TfR is basolateral in WT MDCK cells and other epithelial cells (Fölsch et al., 1999; Gravotta et al., 2007; Hughson and Hopkins, 1990), in spite of possessing the N727-glycan apical signal. Currently available information indicates that TfR expresses two dominant, partially overlapping, basolateral sorting signals in its cytoplasmic domain that direct its basolateral sorting in the biosynthetic and recycling routes (Odorizzi and Trowbridge, 1997). These signals are recognized by the medium subunit of AP-1B at CREs, presumably mediating its incorporation into clathrin-coated vesicles directed to the basolateral plasma membrane (Deborde et al., 2008; Fölsch et al., 1999; Gravotta et al., 2012; Gravotta et al., 2007). The molecular bases of the dominance of basolateral sorting mechanisms over apical sorting mechanism are still unknown. One possibility is that AP-1B operates in a CRE sub-compartment proximal to where the N727-glycan and galectin-4 apical machinery mediates apical transcytosis to ARE. This suggests the interesting possibility that there might be two subdomains in CRE with different sorting functions. Alternatively, both apical and basolateral sorting mechanisms might operate in the same CRE compartment, but AP-1B might be more efficient in capturing the cargo protein prior to sorting. These important questions remain open to future tests using high-temporal resolution trafficking assays that could inform on whether TfR basolateral recycling displays faster kinetics than TfR apical transcytosis. Although we had previously reported that AP-1B KD induced moderate apical missorting of endogenous TfR (Perez Bay et al., 2013), in this report, we observed that apical missorting is higher for the overexpressed TfR, in agreement with many papers using transfected or adenovirus-infected TfR (Ang et al., 2004; Fölsch et al., 1999; Fölsch et al., 2003; Gan et al., 2002; Gravotta et al., 2012; Gravotta et al., 2007). This suggests that cargo overexpression might saturate the apical-basolateral sorting machinery. An additional point that can be stressed is that, because a substantial fraction of TfR (37%) remains basolateral in AP-1B KD MDCK cells, additional (although less efficient) basolateral trafficking mechanisms must contribute to basolateral recycling. The nature of this alternative basolateral sorting machinery remains unknown: it might involve alternative signals and adaptors, such as the Arf6 GAP and effector ACAP1, which has been shown to interact with a sorting signal within the cytoplasmic tail of TfR and regulate its recycling at recycling endosomes in non-polarized cells (Dai et al., 2004).

Our studies also contribute additional evidence that allows further interpretation of the controversial evidence regarding the complementary roles of AP-1B and its highly homologous adaptor AP-1A in basolateral trafficking (Gravotta et al., 2012; Guo et al., 2013; Rodriguez-Boulan et al., 2013). Whereas experimental evidence accumulated over the past decade suggests that AP-1A and AP-1B operate in different subcellular locales, that is, the TGN and CREs, respectively (Fölsch et al., 2003; Gan et al., 2002; Gravotta et al., 2012), it has recently been suggested that these adaptors have identical subcellular localizations, differing mainly in their ability to bind different basolateral cargo proteins (Guo et al., 2013). The results in this report supports the first model because AP-1B is sufficient to mediate efficient basolateral recycling of TfR, whereas AP-1A is not, even when TfR interacts with similar affinity with both AP-1A and AP-1B (Gravotta et al., 2012).

Mechanisms responsible for TfR transcytosis in AP-1B-deficient epithelia

Our studies elucidate the machinery responsible for TfR apicaltranscytosis in AP-1B-deficient epithelia. After TfR

Journal of Cell Science (2014) 127, 4457–4469 doi:10.1242/jcs.153437

internalization from the basolateral plasma membrane, the apical glycan signal linked to N727 and the sorting lectin galectin-4 mediate TfR translocation to ARE and delivery to the apical plasma membrane (Figs 1–3, 5, 6). The galectin-4-mediated apical sorting mechanism might operate by clustering and recruiting TfR molecules into specific lipid microdomains, as this lectin can interact with both glycoproteins and glycolipids (Stechly et al., 2009). The lipid microdomain might serve as a platform for the recruitment of the plus-end kinesin KIF16B, through its PX domain (Hoepfner et al., 2005), which in turn mediates the transport of TfR-containing vesicles from CREs to AREs using a subset of microtubules nucleated in the Golgi complex (Perez Bay et al., 2013; see model in Fig. 7D). The reason why galectin-3 does not mediate TfR apical transcytosis might be due to the fact that this lectin cannot bind glycolipids (Delacour et al., 2007; Stechly et al., 2009); however, we cannot rule out a potential role of this lectin, because its knockdown was partial in our hands. Similar to TfR apical transcytosis, the well-characterized transcytotic pathway of the pIgR depends on microtubules, glycan signals and Rab11a (Apodaca et al., 1994; Luton et al., 2009; Wang et al., 2000), but, in contrast to the apical transcytosis of TfR, it does not require the kinesin KIF16B (Perez Bay et al., 2013) or galectin-4 (this work). This reveals that multiple parallel apical transcytotic pathways exist in epithelial cells.

Functional ablation of either the N727-linked glycan apical signal or galectin-4 inhibits TfR transport to AREs, and increases lysosomal targeting and subsequent degradation, indicating that lysosomal sorting occurs proximally to AREs, either at BSEs or CREs. Although we do not have direct evidence, we believe TfR is delivered to lysosomes from CREs rather than BSEs, because our data consistently shows that TfR localizes in perinuclear endosomes upon ablation of the N727-linked glycan or galectin-4 KD. In addition, only soluble proteins are delivered directly from BSEs to lysosomes through maturation to late endosomes, whereas most recycling receptors, like the TfR, usually escape this pathway and traffic to CREs (Bomsel et al., 1989; Maxfield and McGraw, 2004). Our data showing that ad hoc machinery (i.e. the N727-linked glycan and galectin-4) actively sorts TfR away from the lysosomes in AP-1B KD MDCK cells is in agreement with previous evidence showing that Snx4 prevents TfR lysosomal targeting and degradation in non-polarized cells (Traer et al., 2007).

Implications for translational applications of TfR

The blood–retinal and blood–brain barriers restrict penetration of large biomolecules to the retina and central nervous system, which is key for normal physiology, but remains an obstacle for delivery of therapeutic agents. TfR can be successfully used to deliver to the brain drugs linked to TfR antibodies that reduce the progression of Alzheimer disease (Bell and Ehlers, 2014; Hosoya et al., 2011) through a basolateral transcytotic pathway in brain endothelial cells. Important questions regarding this largely unknown pathway are whether TfR traverses CREs and, if so, which signals and machinery mediate its sorting. Potential candidates include the small GTPase Rab25 and the motor protein MyoVb, which regulate one of the best known basolateral transcytosis pathways, that of the FcRn (Tzaban et al., 2009). By contrast, our studies on TfR apical transcytotis in RPE cells are relevant to drug delivery to the subretinal space, located between the apical plasma membrane of the RPE cells and the photoreceptors. Delivery of VEGF and fluocinolone acetonide to this space for the treatment of wet macular degeneration (Iriyama et al., 2009) and retinitis pigmentosa (Iezzi et al., 2012) can only be achieved by periodical intravitreal injections through the anterior camera of the eye. Drugs conjugated to anti-TfR antibodies could allow these drugs to be administered intravenously, by taking advantage of TfR apical transcytosis in RPE cells.

MATERIALS AND METHODS

Antibodies

The following antibodies were used: rabbit anti-GFP antibody (JM3999; MBL International, Des Plaines, IL), rabbit anti-Rab11a antibody (715300; Invitrogen, Carlsbad, CA), mouse anti-TfR antibody (10R-CD71aHU; Fitzgerald, Acton, MA), mouse anti-HA antibody (MMS-101P; Covance, Princeton, NJ), chicken anti-GAPDH antibody (GW22763; Sigma-Aldrich, St Louis, MO), goat anti-galectin-3 antibody (AF1154. R&D systems), sheep anti-pIgR antibody (secretory component, kindly provided by Keith Mostov, University of California, San Francisco, CA), and Alexa-Fluor-labeled secondary antibodies (Invitrogen, Carlsbad, CA).

Plasmids

T104A, N251A, N317A and N727A mutations in TfR–GFP were generated using WT human TfR fused to GFP in C-terminal domain TfR vector (provided by Tim McGraw, Weill Cornell Medical College, New York, NY), using an Infusion cloning kit (Clontech, Mountain View, CA) and following the manufacturer's instructions.

WT- and N727A-TfR–HA were amplified by PCR from WT and N727A-TfR–GFP vectors and ligated to pcDNA 3.1 Hygro plus plasmid in the *Bam*HI and XhoI sites. The final structure of the plasmids was: pcDNA3.1-*Bam*HI-TfR-HA-XhoI-pcDNA3.1. Reverse oligonucleotides contained the HA sequence. There is no space between TfR and HA. Oligonucleotides used were: FW, 5′-ATCGCGGATCCATGAT-GGATCAAGCTAGATCAGC-3′ and RV, 5′-ATCCGCTCGAGTTAC-GCGTAGTCGGGGACGTCATATGGGTAAAACTCATTGTCAATGT-CCC-3′.

Cell culture

MDCK, LLC-PK1 and ARPE-19 cells were cultured in 5% FBS in DMEM (Invitrogen, Carlsbad, CA). AP-1B KD MDCK cells were selected with 2.5 µg/ml of puromycin (Sigma-Aldrich, St Louis, MO), AP-1B KD/TfR MDCK cells with puromycin and 0.2 mg/ml G418 (Mediatech, Manassas, VA). Cells were plated at 3×10^5 cells in 12-mm Transwell chambers. MDCK and LLC-PK1 were polarized for 4 days and ARPE-19 for 28 days. ARPE-19 in filters were cultured with: 1% FBS in MEM-α, N1 supplement (100×), glutamine-penicillin-streptomycin (100×), nonessential amino acids (100×), hydrocortisone (20 µg/l), taurine (250 mg/l) and triiodo-thyronin (0.013 µg/l) (all from Sigma-Aldrich).

Transfection methods

To transiently knockdown galectin-3 and galectin-4, MDCK and LLC-PK1 4×10^6 cells in suspension cultures were treated with a total of 5 µl siRNA (40 uM) and electroporated with Amaxa Nucleofector kit V (program T23). Two rounds of Amaxa nucleofection separated by 3 days were applied. Canine galectin-3 siRNAs were: 5′-ACCCAAACC-CUCAAGGAUGdTdT-3′ (Delacour et al., 2006) and 5′-AUACCAA-GCUGGAUAAUAUdTdT-3′. Canine galectin-4 siRNA was 5′-GGG-ACAAGGUGGUGUUCAAUU-3′ (Mattila et al., 2012). *Sus scrofa* galectin-4 siRNAs (designed using Dharmacon algorithm) were: $siRNA_1$, 5′-CAGUAAAGGCCCUCAUCCAUU-3′; $siRNA_2$, 5′-CUGGAAAGC-ACAACCAACAUU-3′; $siRNA_3$, 5′-GGACAAAGUGUAUGAACAU-UU-3′. Canine galectin-3 (2.5 µl each) and *Sus scrofa* galectin-4 (1.7 µl each) siRNAs were pooled.

To transiently express WT- and N727A-TfR–GFP in LLC-PK1 cells, the Amaxa nucleofector kit V was used (5 µl plasmid, 1 µg/µl). When LLC-PK1 cells were knocked down for galectin-4 and transfected with WT-TfR–GFP, the corresponding plasmid and siRNAs were applied together during the last Amaxa nucleofection round. To transiently express WT- and N727A-TfR–GFP in MDCK cells, 4 µg of plasmid and

2 µl of lipofectamine per 12-mm filter were applied overnight (10–20% efficiency). To transiently express WT- and N727A-TfR–GFP in ARPE-19 cells, a previously described protocol for electroporation in filters was applied (Deora et al., 2007), using 15 µg of plasmid.

PCR

Galectin-4 and µ1B silencing studies were performed as follows. RNA was extracted from AP-1B KD/TfR MDCK and LLC-PK1 cells plated in 24-well plates using an RNeasy kit (Qiagen, Valencia, CA) on the same day as the immunofluorescence experiment. A one-step RT-PCR (Qiagen, Valencia, CA) was run with 150–200 ng of mRNA per 100 µl reaction for 36 cycles as follows: denaturing step (30 s, 95℃), annealing (30 s, 56℃), polymerization (60 s, 72℃). 50 µl of the reaction was loaded into a 1% agarose gel and run in TAE buffer (25 min, 100 mV). Oligonucleotides were: canine galectin-4, FW, 5′-ACA-TGAGGAGGTTCTGCGTG-3′ and RV, 5′-GGGGATTGAAGTGGAA-GGCA-3′; and canine GAPDH, FW, 5′-GCACAGTCAAGGCTGAG-3′ and RV, 5′-GGGATGACCTTGTCCAC-3′; canine µ1B, previously reported nucleotides (Gravotta et al., 2007); *Sus scrofa* galectin-4, FW, 5′-ACGGTGATCCCTTCTATGAG-3′ and RV, 5-CAGGTTACACGG-CTGTTGG-3′; *Sus scrofa* GAPDH, FW, 5′-GTGTCCTGTGACTT-CAACAG-3′ and RV 5′-TACTCCTTGGAGGCCATGTG-3′.

Western blotting

Cell were incubated in RIPA buffer (30 min, 4℃ with mild shaking) and centrifuged (30 min, 4℃, 16,100 ***g***). ~50 µg of protein samples were loaded in 4–12% gradient polyacrylamide pre-casted gels, ran (90 min, 100 mV) and transferred onto nitrocellulose membrane using iBlot transfer stacks (Invitrogen, Carlsbad, CA).

Degradation assay

WT and AP-1B KD MDCK cells were electroporated with either WT- or N727A-TfR–GFP using Amaxa nucleofection and plated on 24-well plates. Cells were treated with 100 µg/ml cycloheximide for the indicated time, lysed and processed for western blot analysis. WT- and N727A-TfR–GFP expression was identified with anti-TfR antibody, taking advantage of the ~32.7 kDa molecular mass difference between endogenous TfR and TfR–GFP. Quantifications were performed in Image J, by measuring the TfR:GAPDH ratio and normalizing to time 0.

Labeling of transferrin and antibodies

Fe^{3+}-loaded human holo-Tf (Sigma-Aldrich, St Louis, MO), was conjugated with CF594 (Biotium, Hayward, CA) in PBS pH 7.9, using NHS chemistry. A 15× dye:protein molar ratio was used, which yields three fluorophores per Tf molecule. Fluorescent Tf was purified three times with 50-kDa cut-off centrifugal filters (Milipore). CF594–Tf had been previously validated as a ligand for TfR through fluorescence microscopy experiments showing its co-localization with anti-TfR antibody and through competition experiments that showed inhibition of CF594–Tf uptake by the presence of 200× unlabeled Tf (Perez Bay et al., 2013). Anti-GFP and anti-HA antibodies were labeled with SeTau647 (SETA Biomedicals, Urbana, IL) following the same procedure.

Microscopy

Images were collected with a Zeiss Axio Observer inverted microscope, Yokogawa Confocal Scanner Unit CSU-X1, Rolera EMCCD and AxioCam-503 CCD cameras and Zeiss planapochromat 63×/1.4 NA oil-immersion objective. Data analysis was performed with Axiovision Rel. 4.8 and Zen (Zeiss, Oberkochen, Germany) software.

Surface immunofluorescence

Polarized cells on 12-mm Transwell filters were fixed with 4% PFA in PBS (room temperature, 10 min), incubated with 50 mM NH_4Cl^- in PBS (room temperature, 15 min) and blocked with 1% BSA in PBS (room temperature, 120 min). Primary antibodies (against GFP or TfR) were added at 1:500 in 1% BSA in PBS (4℃, overnight). Because cells were not permeabilized and the antibodies recognized luminal epitopes, only plasma membrane proteins were labeled in this step. After three washes with 1% BSA in PBS (room temperature, 20 min), Alexa-Fluor-647- and Alexa-Fluor-568-labeled secondary antibodies were, respectively, applied to the apical or basolateral chambers 1:500 in 1% BSA in PBS (4℃, 3 h) and washed three times with 1% BSA in PBS (room temperature, 20 min). Filters were not removed from the case until the end of the last wash to avoid mixing of the secondary antibodies.

Transcytosis assay

WT and AP-1B KD MDCK cells plated on 12-mm Transwell filters were transiently transfected at day 3 with either WT- or N727-TfR–GFP. At day 4, cells were serum starved in 20 mM HEPES in HBSS (37℃, 60 min), incubated basolaterally with 2.5 ug/ml SeTau647-labeled rabbit anti-GFP antibody in HEPES in HBSS (4℃, 120 min) and rinsed three times with HEPES in HBSS (4℃). The temperature was witched to 37℃ for 0, 5-, 15- or 30-min periods, during which Alexa-Fluor-568-conjugated anti-rabbit-IgG antibody was applied apically. After rinsing three times with HEPES in HBSS (4℃), cells were fixed with 4% PFA in PBS (4℃, 10 min), incubated with 50 mM NH_4Cl^- in PBS (room temperature, 15 min) and mounted for imaging.

Anti-HA and transferrin antibody uptake assay

AP-1B KD MDCK and AP-1B KD/TfR MDCK cells were plated on 12-mm Transwell filters. The former were transiently transfected at day 3 with either WT- or N727-TfR–HA. At day 4, cells were serum starved in 20 mM HEPES in HBSS (37℃, 60 min) and incubated basolaterally with 2.5 µg/ml SeTau647-labeled mouse anti-HA antibody (4℃, 120 min, HEPES in HBSS) or 5 µg/ml CF594–Tf (4℃, 60 min, 1%BSA in HBSS). After switching temperature for the indicated times, cells were fixed with 4% PFA in PBS (4℃, 10 min) and processed for immunofluorescence.

Quantification, colocalization analysis and statistics

The apical:basolateral ratio was calculated with the following method. The apical and basolateral TfR fluorescence were quantified by multiplying the mean intensity fluorescence (MIF) and the number of pixels (total fluorescence=*MIF*×area) of each region of interest (i.e. one cell) and summed for each section of the confocal stack. This provides the total amount of apical and basolateral TfR fluorescence per cell. Then, the apical:basolateral ratio was obtained. The use of two secondary antibodies provides an objective criteria to identify the apical and basolateral TfR, which is difficult to determine when using only one secondary antibody; however, this method does not indicate the absolute amount of TfR in each domain due to the different quantum yield associated to the two fluorophores used. For this reason, values were normalized to control and changes in the apical:basolateral ratio were determined among different conditions studied.

Colocalization was quantified with the Manders' coefficients, which constitute the most accepted method to measure colocalization between different cellular markers A and B (Dunn et al., 2011). To determine the area of marker 'A' (i.e. Rab11a) occupied by marker 'B' (i.e. TfR), we quantified the pixels of marker A colocalizing with marker B divided by the total pixels of marker A. This operation was applied for all the confocal sections of a confocal stack in each region of interest (i.e. one cell). The inverse formula was utilized to calculate the area of marker B occupied by marker A.

Statistics

Values are expressed as mean±s.e.m. The statistical method used was the Student's *t*-test. The levels of statistical significance are specified for each comparison in the respective figure.

Acknowledgements

We gratefully acknowledge Keith Mostov and Tim McGraw for valuable reagents.

Competing interests

The authors declare no competing interests.

Author contributions

A.P.B., R.S. and I.B. conducted experiments. A.P.B., R.S., I.B. and E.R.-B. were responsible for experimental design and data interpretation, and A.P.B. and E.R.-B. for writing.

Funding

This work was supported by the National Institutes of Health (NIH) [grant numbers GM34107 and EY08538 to E.R.-B., and a K01 award 1K01DK102836-01 to A.P.B.]; the Research to Prevent Blindness Foundation; and the Dyson Foundation. Deposited in PMC for release after 12 months.

Supplementary material

Supplementary material available online at
http://jcs.biologists.org/lookup/suppl/doi:10.1242/jcs.153437/-/DC1

References

Ang, A. L., Taguchi, T., Francis, S., Fölsch, H., Murrells, L. J., Pypaert, M., Warren, G. and Mellman, I. (2004). Recycling endosomes can serve as intermediates during transport from the Golgi to the plasma membrane of MDCK cells. *J. Cell Biol.* **167**, 531-543.

Apodaca, G., Katz, L. A. and Mostov, K. E. (1994). Receptor-mediated transcytosis of IgA in MDCK cells is via apical recycling endosomes. *J. Cell Biol.* **125**, 67-86.

Bell, R. D. and Ehlers, M. D. (2014). Breaching the blood-brain barrier for drug delivery. *Neuron* **81**, 1-3.

Bomsel, M., Prydz, K., Parton, R. G., Gruenberg, J. and Simons, K. (1989). Endocytosis in filter-grown Madin-Darby canine kidney cells. *J. Cell Biol.* **109**, 3243-3258.

Bonifacino, J. S. (2014). Adaptor proteins involved in polarized sorting. *J. Cell Biol.* **204**, 7-17.

Chen, R., Jiang, X., Sun, D., Han, G., Wang, F., Ye, M., Wang, L. and Zou, H. (2009). Glycoproteomics analysis of human liver tissue by combination of multiple enzyme digestion and hydrazide chemistry. *J. Proteome Res.* **8**, 651-661.

Dai, J., Li, J., Bos, E., Porcionatto, M., Premont, R. T., Bourgoin, S., Peters, P. J. and Hsu, V. W. (2004). ACAP1 promotes endocytic recycling by recognizing recycling sorting signals. *Dev. Cell* **7**, 771-776.

Deborde, S., Perret, E., Gravotta, D., Deora, A., Salvarezza, S., Schreiner, R. and Rodriguez-Boulan, E. (2008). Clathrin is a key regulator of basolateral polarity. *Nature* **452**, 719-723.

Delacour, D., Cramm-Behrens, C. I., Drobecq, H., Le Bivic, A., Naim, H. Y. and Jacob, R. (2006). Requirement for galectin-3 in apical protein sorting. *Curr. Biol.* **16**, 408-414.

Delacour, D., Greb, C., Koch, A., Salomonsson, E., Leffler, H., Le Bivic, A. and Jacob, R. (2007). Apical sorting by galectin-3-dependent glycoprotein clustering. *Traffic* **8**, 379-388.

Deora, A. A., Diaz, F., Schreiner, R. and Rodriguez-Boulan, E. (2007). Efficient electroporation of DNA and protein into confluent and differentiated epithelial cells in culture. *Traffic* **8**, 1304-1312.

Diaz, F., Gravotta, D., Deora, A., Schreiner, R., Schoggins, J., Falck-Pedersen, E. and Rodriguez-Boulan, E. (2009). Clathrin adaptor AP1B controls adenovirus infectivity of epithelial cells. *Proc. Natl. Acad. Sci. USA* **106**, 11143-11148.

Dunn, K. W., Kamocka, M. M. and McDonald, J. H. (2011). A practical guide to evaluating colocalization in biological microscopy. *Am. J. Physiol.* **300**, C723-C742.

Fiedler, K. and Simons, K. (1995). The role of N-glycans in the secretory pathway. *Cell* **81**, 309-312.

Fölsch, H. (2008). Regulation of membrane trafficking in polarized epithelial cells. *Curr. Opin. Cell Biol.* **20**, 208-213.

Fölsch, H., Ohno, H., Bonifacino, J. S. and Mellman, I. (1999). A novel clathrin adaptor complex mediates basolateral targeting in polarized epithelial cells. *Cell* **99**, 189-198.

Fölsch, H., Pypaert, M., Maday, S., Pelletier, L. and Mellman, I. (2003). The AP-1A and AP-1B clathrin adaptor complexes define biochemically and functionally distinct membrane domains. *J. Cell Biol.* **163**, 351-362.

Gan, Y., McGraw, T. E. and Rodriguez-Boulan, E. (2002). The epithelial-specific adaptor AP1B mediates post-endocytic recycling to the basolateral membrane. *Nat. Cell Biol.* **4**, 605-609.

Gonzalez, A. and Rodriguez-Boulan, E. (2009). Clathrin and AP1B: key roles in basolateral trafficking through trans-endosomal routes. *FEBS Lett.* **583**, 3784-3795.

Gravotta, D., Deora, A., Perret, E., Oyanadel, C., Soza, A., Schreiner, R., Gonzalez, A. and Rodriguez-Boulan, E. (2007). AP1B sorts basolateral proteins in recycling and biosynthetic routes of MDCK cells. *Proc. Natl. Acad. Sci. USA* **104**, 1564-1569.

Gravotta, D., Carvajal-Gonzalez, J. M., Mattera, R., Deborde, S., Banfelder, J. R., Bonifacino, J. S. and Rodriguez-Boulan, E. (2012). The clathrin adaptor AP-1A mediates basolateral polarity. *Dev. Cell* **22**, 811-823.

Guo, X., Mattera, R., Ren, X., Chen, Y., Retamal, C., González, A. and Bonifacino, J. S. (2013). The adaptor protein-1 μ1B subunit expands the repertoire of basolateral sorting signal recognition in epithelial cells. *Dev. Cell* **27**, 353-366.

Hoepfner, S., Severin, F., Cabezas, A., Habermann, B., Runge, A., Gillooly, D., Stenmark, H. and Zerial, M. (2005). Modulation of receptor recycling and degradation by the endosomal kinesin KIF16B. *Cell* **121**, 437-450.

Hosoya, K., Tomi, M. and Tachikawa, M. (2011). Strategies for therapy of retinal diseases using systemic drug delivery: relevance of transporters at the blood-retinal barrier. *Expert Opin. Drug Deliv.* **8**, 1571-1587.

Hughes, R. C. (1999). Secretion of the galectin family of mammalian carbohydrate-binding proteins. *Biochim. Biophys. Acta* **1473**, 172-185.

Hughson, E. J. and Hopkins, C. R. (1990). Endocytic pathways in polarized Caco-2 cells: identification of an endosomal compartment accessible from both apical and basolateral surfaces. *J. Cell Biol.* **110**, 337-348.

Hunt, R. C., Dewey, A. and Davis, A. A. (1989). Transferrin receptors on the surfaces of retinal pigment epithelial cells are associated with the cytoskeleton. *J. Cell Sci.* **92**, 655-666.

Iezzi, R., Guru, B. R., Glybina, I. V., Mishra, M. K., Kennedy, A. and Kannan, R. M. (2012). Dendrimer-based targeted intravitreal therapy for sustained attenuation of neuroinflammation in retinal degeneration. *Biomaterials* **33**, 979-988.

Iriyama, A., Inoue, Y., Takahashi, H., Tamaki, Y., Jang, W. D. and Yanagi, Y. (2009). A2E, a component of lipofuscin, is pro-angiogenic in vivo. *J. Cell. Physiol.* **220**, 469-475.

Jacob, R., Alfalah, M., Grünberg, J., Obendorf, M. and Naim, H. Y. (2000). Structural determinants required for apical sorting of an intestinal brush-border membrane protein. *J. Biol. Chem.* **275**, 6566-6572.

Luton, F., Hexham, M. J., Zhang, M. and Mostov, K. E. (2009). Identification of a cytoplasmic signal for apical transcytosis. *Traffic* **10**, 1128-1142.

Mattila, P. E., Youker, R. T., Mo, D., Bruns, J. R., Cresawn, K. O., Hughey, R. P., Ihrke, G. and Weisz, O. A. (2012). Multiple biosynthetic trafficking routes for apically secreted proteins in MDCK cells. *Traffic* **13**, 433-442.

Maxfield, F. R. and McGraw, T. E. (2004). Endocytic recycling. *Nat. Rev. Mol. Cell Biol.* **5**, 121-132.

Mellman, I. and Nelson, W. J. (2008). Coordinated protein sorting, targeting and distribution in polarized cells. *Nat. Rev. Mol. Cell Biol.* **9**, 833-845.

Mishra, R., Grzybek, M., Niki, T., Hirashima, M. and Simons, K. (2010). Galectin-9 trafficking regulates apical-basal polarity in Madin-Darby canine kidney epithelial cells. *Proc. Natl. Acad. Sci. USA* **107**, 17633-17638.

Mostov, K. E., Verges, M. and Altschuler, Y. (2000). Membrane traffic in polarized epithelial cells. *Curr. Opin. Cell Biol.* **12**, 483-490.

Nickel, W. (2005). Unconventional secretory routes: direct protein export across the plasma membrane of mammalian cells. *Traffic* **6**, 607-614.

Odorizzi, G. and Trowbridge, I. S. (1997). Structural requirements for basolateral sorting of the human transferrin receptor in the biosynthetic and endocytic pathways of Madin-Darby canine kidney cells. *J. Cell Biol.* **137**, 1255-1264.

Ohno, H., Tomemori, T., Nakatsu, F., Okazaki, Y., Aguilar, R. C., Foelsch, H., Mellman, I., Saito, T., Shirasawa, T. and Bonifacino, J. S. (1999). Mu1B, a novel adaptor medium chain expressed in polarized epithelial cells. *FEBS Lett.* **449**, 215-220.

Perez Bay, A. E., Schreiner, R., Mazzoni, F., Carvajal-Gonzalez, J. M., Gravotta, D., Perret, E., Lehmann Mantaras, G., Zhu, Y. S. and Rodriguez-Boulan, E. J. (2013). The kinesin KIF16B mediates apical transcytosis of transferrin receptor in AP-1B-deficient epithelia. *EMBO J.* **32**, 2125-2139.

Poland, P. A., Rondanino, C., Kinlough, C. L., Heimburg-Molinaro, J., Arthur, C. M., Stowell, S. R., Smith, D. F. and Hughey, R. P. (2011). Identification and characterization of endogenous galectins expressed in Madin Darby canine kidney cells. *J. Biol. Chem.* **286**, 6780-6790.

Rodriguez-Boulan, E. and Macara, I. G. (2014). Organization and execution of the epithelial polarity programme. *Nat. Rev. Mol. Cell Biol.* **15**, 225-242.

Rodriguez-Boulan, E., Kreitzer, G. and Müsch, A. (2005). Organization of vesicular trafficking in epithelia. *Nat. Rev. Mol. Cell Biol.* **6**, 233-247.

Rodriguez-Boulan, E., Perez-Bay, A., Schreiner, R. and Gravotta, D. (2013). Response: the ''tail'' of the twin adaptors. *Dev. Cell* **27**, 247-248.

Scheiffele, P., Roth, M. G. and Simons, K. (1997). Interaction of influenza virus haemagglutinin with sphingolipid-cholesterol membrane domains via its transmembrane domain. *EMBO J.* **16**, 5501-5508.

Schreiner, R., Frindt, G., Diaz, F., Carvajal-Gonzalez, J. M., Perez Bay, A. E., Palmer, L. G., Marshansky, V., Brown, D., Philp, N. J. and Rodriguez-Boulan, E. (2010). The absence of a clathrin adapter confers unique polarity essential to proximal tubule function. *Kidney Int.* **78**, 382-388.

Stechly, L., Morelle, W., Dessein, A. F., André, S., Grard, G., Trinel, D., Dejonghe, M. J., Leteurtre, E., Drobecq, H., Trugnan, G. et al. (2009). Galectin-4-regulated delivery of glycoproteins to the brush border membrane of enterocyte-like cells. *Traffic* **10**, 438-450.

Straube, T., von Mach, T., Hönig, E., Greb, C., Schneider, D. and Jacob, R. (2013). pH-dependent recycling of galectin-3 at the apical membrane of epithelial cells. *Traffic* **14**, 1014-1027.

Traer, C. J., Rutherford, A. C., Palmer, K. J., Wassmer, T., Oakley, J., Attar, N., Carlton, J. G., Kremerskothen, J., Stephens, D. J. and Cullen, P. J. (2007). SNX4 coordinates endosomal sorting of TfnR with dynein-mediated transport into the endocytic recycling compartment. *Nat. Cell Biol.* **9**, 1370-1380.

Tzaban, S., Massol, R. H., Yen, E., Hamman, W., Frank, S. R., Lapierre, L. A., Hansen, S. H., Goldenring, J. R., Blumberg, R. S. and Lencer, W. I. (2009). The recycling and transcytotic pathways for IgG transport by FcRn are distinct and display an inherent polarity. *J. Cell Biol.* **185**, 673-684.

Wang, X., Kumar, R., Navarre, J., Casanova, J. E. and Goldenring, J. R. (2000). Regulation of vesicle trafficking in madin-darby canine kidney cells by Rab11a and Rab25. *J. Biol. Chem.* **275**, 29138-29146.

Weisz, O. A. and Rodriguez-Boulan, E. (2009). Apical trafficking in epithelial cells: signals, clusters and motors. *J. Cell Sci.* **122**, 4253-4266.

Yeaman, C., Le Gall, A. H., Baldwin, A. N., Monlauzeur, L., Le Bivic, A. and Rodriguez-Boulan, E. (1997). The O-glycosylated stalk domain is required for apical sorting of neurotrophin receptors in polarized MDCK cells. *J. Cell Biol.* **139**, 929-940.